small methods
www.small-methods.com

Photothermal Membrane Distillation toward Solar Water Production

*Minmin Gao, Connor Kangnuo Peh, Fan Lu Meng, and Ghim Wei Ho**

Freshwater production is one of the biggest global challenges today. Though desalination can provide a climate-independent source of clean water, the process requires a high energy consumption. Emerging advancement of photothermal nanomaterials and the urgent demand for a green technology transition have reinvigorated the established solar distillation technology. The current development of photothermal vaporization focuses on material innovation and interfacial heating, which largely emphasizes vapor generation efficiency, without considering pragmatic water collection. Moreover, salt accumulation is another critical issue of seawater solar-driven vaporization. The incorporation of photothermal materials into a photothermal membrane distillation (PMD) solar evaporator design harmoniously resolves these issues through combination of renewable energy and efficient interfacial distillation, to achieve the ultimate goal of practical saline water into freshwater conversion. At this juncture, it is imperative to review the recent opportunities and progresses of the PMD system. Here, the fundamental photothermal processes, strategies for efficient evaporator design, evaluation of various criteria for photothermal material incorporation with desired properties, discussions on desalination, water treatment, and energy generation applications are covered. Guidelines in material and system designs to further advance the PMD system that is highly promising in delivering portable water for both large-scale and decentralized systems are provided.

1. Introduction

The continuous supply of safe, clean and affordable water is essential for human well-being and sustainable development. Currently, 3.9 billion people are living under conditions of severe physical water scarcity for at least one month per year according to the United Nations (World Water Development Report 2020). Such a situation will become worse with climate change, pollution, population growth and rapid urbanization. Studies have predicted by 2050, around 52% of the world's population is likely to live in water-stressed conditions.[1] As 97% of the Earth's surface water is in the ocean, desalination that turns seawater into freshwater, plays a critical role in tackling the issue of depleting freshwater supplies. However, desalination and water treatment often involve intensive energy consumption, which also augment the emission of greenhouse gases. Solar-driven distillation that is powered by the widely available and abundant solar energy is a viable solution for energy-efficient and CO_2-free freshwater production, and consequently reconciles the water-energy nexus. Moreover, the fast development of photothermal nanomaterials with efficient solar-to-thermal conversion, reinvigorates solar-assisted desalination to become one of the most promising and attractive technology for freshwater production in the outlook of sustainability.

Traditional solar vaporization system involves volumetric heating with large thermal mass and significant heat loss. The advances in nanostructured photothermal materials and interfacial evaporator designs realize a highly localized photothermal heating at the evaporation surface, which maximizes solar utilization and suppresses heat loss to the bulk water.[17–20] However, the high vaporization rate does not necessarily translate to efficient water harvesting, given that the evaporation rate is mainly calculated by mass loss of water in the open ambient without an effective water collection system.[21] Recent review articles also revealed the limitation of novel materials in further enhancing the solar evaporation efficiency, while identified system design-based approach offers significant opportunity in augmenting the overall energy efficiency of desalination technologies.[22–24] Some researchers have incorporated a simple solar still with the photothermal active material in an enclosed condensation chamber. The chamber design typically consists of a transparent condensing surface in various constrained geometries, such as inclined flat surface,[7,25] conical,[26] quasi-semispherical,[27,28] rooftop,[3,8,25] and pyramid.[3,29] These conventional interfacial designs (**Figure 1**a) though simple and economical, the major drawback faced is the limited water collection efficiency resulting from inevitable high humidity entrapped within the chamber, interference of light harvesting by the condensate/vapor, and heating up of the condensing surface over time.

Dr. M. Gao, Dr. C. K. Peh, Dr. F. L. Meng, Prof. G. W. Ho
Department of Electrical and Computer Engineering
National University of Singapore
4 Engineering Drive 3, Singapore 117583, Singapore
E-mail: elehgw@nus.edu.sg
Prof. G. W. Ho
Institute of Materials Research and Engineering
A*STAR (Agency for Science, Technology and Research)
2 Fusionopolis Way, Singapore 138634, Singapore
The ORCID identification number(s) for the author(s) of this article can be found under https://doi.org/10.1002/smtd.202001200.

DOI: 10.1002/smtd.202001200

Mitigation efforts have been made to direct the generated vapor to a separated chamber for condensation, such as introducing a solar-powered electrical fan.[2] Nevertheless, the vapor-to-distillate conversion efficiency of the solar stills remains generally low, while other designs with complicated device configurations are less practical and cost effective.

The emerging pursuit to introduce a hydrophobic microporous membrane that completely separates the water and the condensate, bypasses these limitations of the conventional solar stills, and allows viable water collection as the generated vapor moves in an opposing direction from the incident light path and condenses on the other side. This solar evaporator configuration with photothermal membrane distillation (PMD) design (Figure 1b) thereby achieves a relatively higher vapor-to-distillate conversion efficiency (Figure 1c).[30] Moreover, this configuration in conjunction with thermal recycling could drive the overall solar-to-distillate conversion efficiency of the system far exceeds the thermodynamic theoretical limit with multi-fold enhancement.[11,14,31,32] The localized heating at the evaporation surface enhances the thermal efficiency and substantially reduces energy input needed for bulk heating of the feed.[33] Besides, it possesses the advantages of the conventional membrane distillation (MD) system over other desalination techniques, such as the ability to treat high-salinity waters, wide operating conditions, i.e., low-grade heat and low-pressure, reduced fouling issues, and highly compact design.[34] Therefore, the PMD technology (Figure 1b) is promising for next-generation portable water solutions with reduced energy consumption, especially for remote off-grid regions.[35–37]

Herein, the review begins with the introduction of fundamental processes involved in the PMD system including photothermal conversion, vaporization and condensation, followed by system classifications and the core criteria of light harvesting, thermal management and condenser design on system-level, as well as material innovation on microscopic-level for achieving efficient PMD system (**Figure 2**). Specifically, the efficiency of PMD concerning localized interfacial heating, light distribution, temperature polarization, thermal resistance

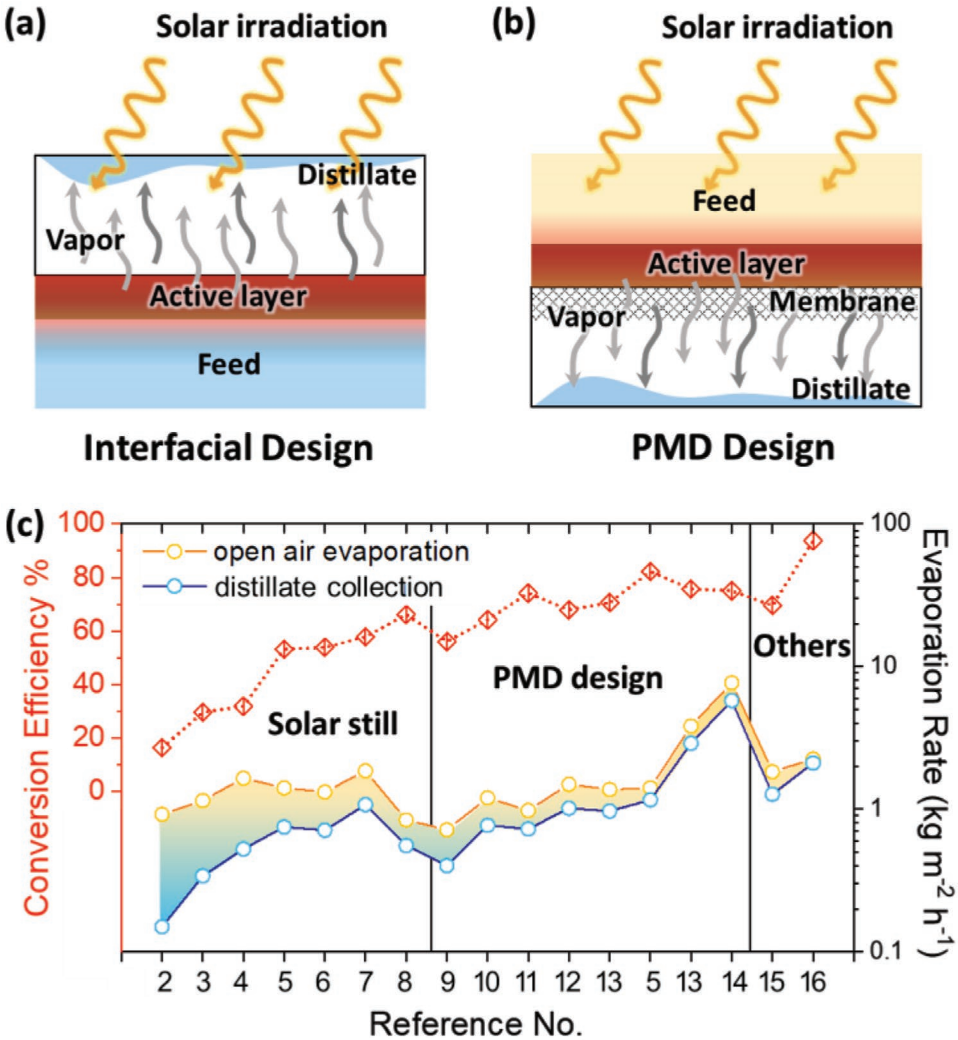

Figure 1. a) Solar vaporization using the interfacial design with conventional solar still for distillate collection. b) Solar vaporization using a PMD design with membrane distillation configuration for distillate collection. c) Comparison of vapor-to-distillate conversion efficiency with various design configurations.[2–16]

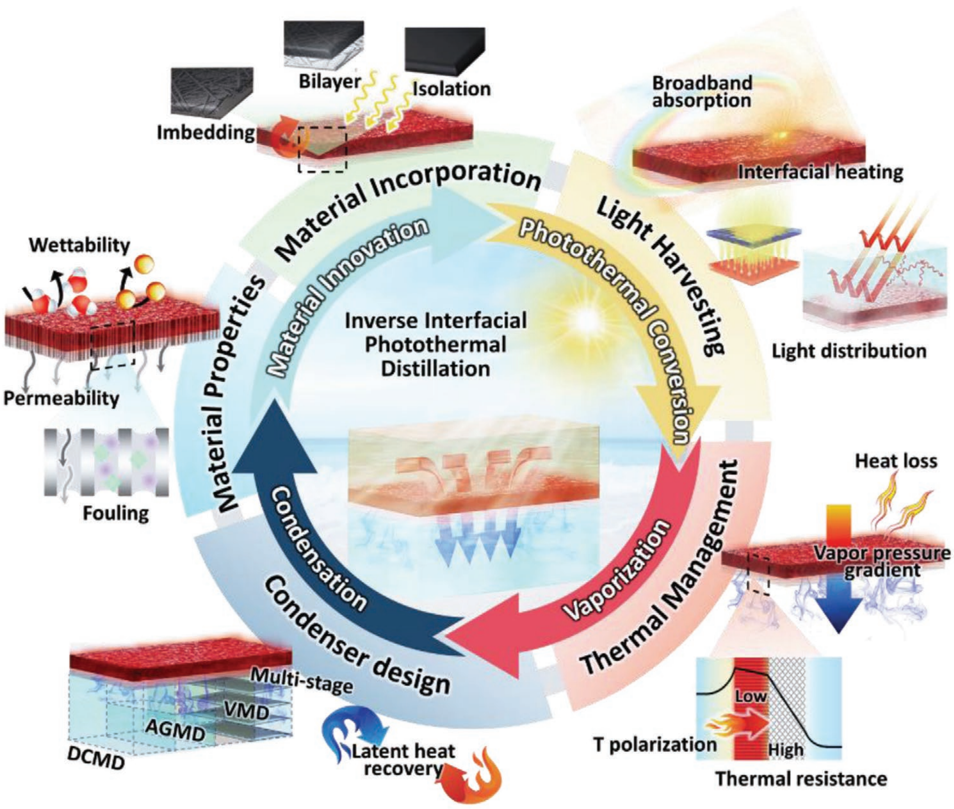

Figure 2. Schematic drawing of the scope of this photothermal membrane distillation review.

and insulation, as well as latent heat recovery in various systems will be comprehensively evaluated. Also, various aspects regarding photothermal active layer design will be discussed, including material innovation and incorporation, and their photothermal properties, wettability, permeability and durability. Moreover, the recent development in the PMD system is reviewed in relation to their practical application in desalination, water treatment and energy generation. Finally, conclusion and perspective of the PMD system are presented. This review offers an overview of the emerging trend in strategic incorporation of the photothermal nanomaterials in membrane distillation for practical, continuous and upscaling water collection prospects. It also provides a guide for designing desirable photothermal materials and efficient PMD systems, and inspires potential research directions for solar-driven water-energy applications.

2. Fundamental Processes

Generally, the feed solution in the PMD system is separated from the distillate using a hydrophobic microporous membrane as in the conventional MD system. Upon solar irradiation, the photothermal active layer in the PMD system provides a localized heating at the evaporation surface. The increase in temperature at the evaporation surface enhances the partial vapor pressure gradient across the membrane which is the driving force for vapor permeation. After the vapor passing through the membrane, distillate is collected through condensation on the other side of the membrane. The PMD system involves mainly three conversion processes (**Figure 3**a): 1) photothermal process that converts light to heat which is governed by the photothermal effect of nanomaterials; 2) vaporization process that transforms water into vapor phase which is associated to the thermal efficiency of generated heat used for vaporization; and 3) condensation process that translates vapor into distillate based on various condenser designs. Therefore, in the design of an efficient PMD system, both the solar-to-thermal conversion capability of the photothermal nanomaterials and the intrinsic characteristics of the PMD configuration contribute to its overall performance. The fundamental mechanisms and relevant calculations are presented in this section to provide theoretical and quantitative framework for understanding the overall performance of the PMD system.

2.1. Photothermal Conversion

In a PMD system, the photothermal materials play an important role in converting solar energy to heat. Various types of photothermal materials have been studied, including metallic materials, semiconductors, as well as carbon-based materials. These engineered materials will absorb the incoming radiation from the sun, and convert them into heat through hot electron generation from plasmonic resonance, non-radiative relaxation of photoexcited electrons, molecular or lattice vibration or other means.[38–42] A major factor of how much heat energy can convert from light energy is determined by how well the

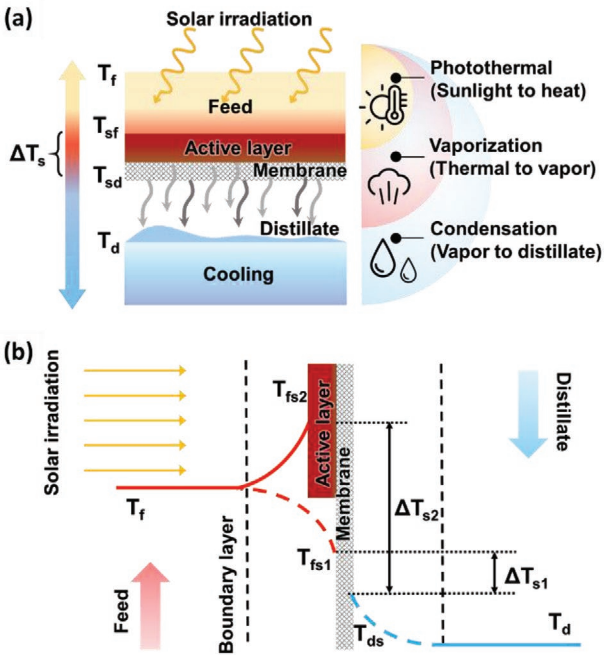

Figure 3. a) Schematic illustration showing the mechanism of PMD and b) its effect on temperature polarization compared to conventional MD.

photothermal material can absorb solar radiation. This is often measured by the solar absorptance, which is determined by the ratio of the total absorbed solar radiation to the incident radiation. The total solar absorptance $\alpha(\theta)$ of a material for a given angle of incidence θ is the weighted average of the spectral absorptance of the material over the spectral irradiance distribution of the standard solar spectrum (AM 1.5), as described in the equation below[43]

$$\alpha(\theta) = \frac{\int_{\lambda_{\min}}^{\lambda_{\max}} [1-R(\theta,\lambda)]A(\theta,\lambda)d\lambda}{\int_{\lambda_{\min}}^{\lambda_{\max}} A(\lambda)d\lambda} \tag{1}$$

where $\lambda_{\min}$ and $\lambda_{\max}$ are 300 and 2500 nm respectively, and θ is the angle of incidence of light measured from the surface normal of the absorber. $A(\lambda)$ is the wavelength-dependent solar spectral irradiance and $R(\theta, \lambda)$ is the total reflectance at wavelength λ.

2.2. Photothermal Membrane Distillation

The conventional MD system is a hybrid thermal-membrane technology. The preheated feed solution is separated from the cold distillate with a microporous hydrophobic membrane. The hydrorepellent nature of the membrane prevents liquid filtration, while mass transfer only takes place in the vapor phase driven by the temperature-induced partial vapor pressure gradient across the membrane. In principle, nonvolatile solutes, such as macromolecules, colloids and ions, are completely rejected.[44] The low hydrostatic pressure on the membrane helps to minimize fouling, making MD suitable for hypersaline or highly polluted wastewater treatment.[21] Moreover, MD can be operated with low-grade heat (≈50–80 °C), making it less energy-intensive.[44] The photothermal active layer in the PMD system provides a localized heating at the evaporation surface, thus enhancing the driving force for vapor permeation, further reducing the energy required for heating the feed.

This vapor generation process in membrane distillation can be described with the following equation[35,37,45]

$$J_{\text{vapor}} = k\left[P_{\text{v,f}}\left(S, T_{\text{ds}} + \Delta T_{\text{s}}\right) - P_{\text{v,d}}\left(0, T_{\text{ds}}\right)\right] \tag{2}$$

where J_{vapor} is the vapor flux, k is the permeability coefficient of the membrane that is related to its properties, such as porosity and thickness. $P_{\text{v,f}}$ $(S,\ T_{\text{ds}} + \Delta T_{\text{s}})$ is the partial vapor pressure of the feed with salinity S at temperature $T_{\text{ds}} + \Delta T_{\text{s}}$, where ΔT_{s} is the transmembrane temperature difference (Figure 3b). $P_{\text{v,d}}$ $(0,\ T_{\text{ds}})$ is the partial vapor pressure of the distillate at temperature T_{ds}.

One of the main challenges of conventional MD is the temperature polarization (Figure 3b). The temperature at the feed-membrane interface (or evaporation surface) is lower than the bulk feed ($T_{\text{fs1}} < T_{\text{f}}$) due to evaporation and heat loss. Consequently, the transmembrane temperature difference (ΔT_{s1}) is reduced, so do the driving force and the overall efficiency.[46] Introducing photothermal nanomaterials induces highly localized heating at the feed-membrane interface. The interface temperature is higher than the bulk ($T_{\text{fs2}} > T_{\text{f}}$) which reduces the temperature polarization effect ($\Delta T_{\text{s2}} > \Delta T_{\text{s1}}$), thus improves the thermal efficiency.

The last process is condensation, with its efficiency expressed by gained output ratio (GOR) that is defined as the number of kilograms of distillate produced per kilogram of vapor

$$\text{GOR} = \frac{m_{\text{distillate}}}{m_{\text{vapor}}} \tag{3}$$

A system without latent heat recovery (i.e., max GOR = 1), even with the increase of the efficiency of the first two processes (photothermal conversion and vaporization) to their maximum (i.e., 100%), can only improve the overall efficiency to a limited extent. The GOR of a well-designed thermal distillation system should be greater than one, thus leading to multi-fold enhancement depending on the effectiveness of latent heat recovery.[36]

The overall solar-to-distillate efficiency of the PMD system can be calculated based on the equation below[47,48]

$$\eta_{\text{solar-distillate}} = J_{\text{distillate}}\left(h_{\text{lv}} + C\left(T_{\text{fs}} - T_{\text{f}}\right)\right)/P_{\text{in}} \tag{4}$$

Where $J_{\text{distillate}}$ is the permeate flux across the membrane, h_{lv} is the water evaporation enthalpy, $C(T_{\text{fs}} - T_{\text{f}})$ is the heat required to increase the feed temperature at the membrane surface from T_{f} to T_{fs} with the specific heat of water C (4.2 kJ kg^{-1} K^{-1}), P_{in} is the incident power density of solar irradiation. In the passive solar distillation system, the overall system efficiency is the same as $\eta_{\text{solar-distillate}}$. In the case of external energy is supplied, such as pumping or preheating the feed, the overall system efficiency should take consideration of the total input energy.

3. System Classifications

PMD systems can be classified into four categories (**Figure 4**), according to the positions of the photothermal active layer in the liquid feed media and the condenser configuration. The first three systems are active crossflow system, which are similar to conventional MD systems, namely direct contact (Figure 4a), air-gap (Figure 4b) and vacuum (Figure 4c) membrane distillation systems, with the photothermal active layer placed right at the evaporation interface. In the last system, the photothermal active layer is separated from the feed with incorporated latent heat recovery design which is referred as the multi-stage system (Figure 4d). In this configuration, passive system can be realized using dead-end water or water wicking through the hydrophilic layer as the feed water supply. In the latter case, membrane-free system with a small air gap between the hydrophilic layers can be used for liquid layer separation (Figure 4dii).[31]

The performances of various PMD systems shown significant enhancement compared with the system without the photothermal active layer under the same conditions (**Figure 5**). Moreover, the demonstrated improvement in permeate flux ranges from ≈2 to 5.5 times higher under low solar irradiation (≤1 sun), and ≈6 to 20 times under high solar power density. Generally, the higher the light irradiation intensity, the more effective is the photothermal active layer to reach a higher temperature (T_{fs}). For instance, Jun's group[46] demonstrated that the interface temperature increased by 6 and 12 °C in the presence of the photothermal active layer under 0.75 and 7 suns respectively. The higher temperature leads to an improved permeate rate (>19 times) under 7 suns, but the solar conversion efficiency was lower (41%) compared to the case with 0.75 sun (45%) due to high optical power input. Furthermore, in the cases where the external energy is supplied for pumping or preheating the feed, the overall solar-to-distillate efficiency of the system should include these energy inputs besides solar irradiation.

4. Strategies for Efficient PMD System

As discussed, the overall energy efficiency of the PMD system is based on the three conversion processes, from light to heat, subsequently to vapor and then finally to distillate. The first process is governed by both the intrinsic properties of the photothermal materials and the light utilization across the active area. Subsequently, the photoconverted thermal energy needs to be applied at the desired location with minimum heat loss to obtain a high transmembrane temperature gradient (ΔT_s). This drives the mass transfer of the generated vapor across the membrane to the lower temperature side. Finally, the vapor can be condensed and collected as distillate. Every process is crucial and indispensable for the overall efficiency of the PMD system. In this section, we will discuss different strategies for achieving efficient PMD based on their system designs, in terms of light harvesting, thermal management, and condenser design, primarily on a system-level.

4.1. Light Harvesting

Photothermal conversion from solar energy is a direct conversion process that possesses the utmost attainable conversion efficiency.[50] The development of nanostructured photothermal materials is an emerging approach for solar freshwater production. The advantages of the nanostructured material encompass

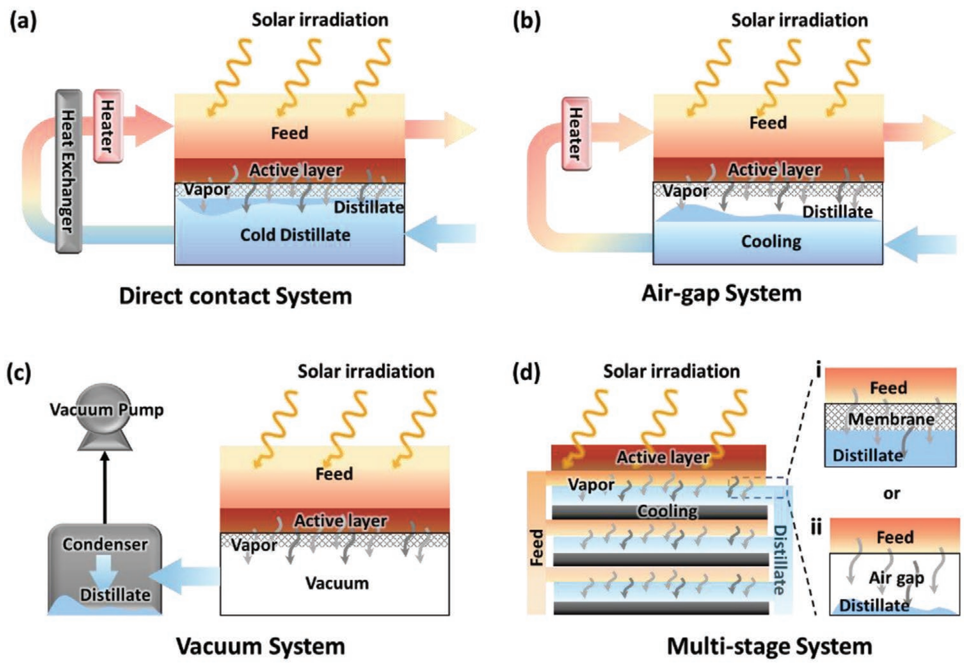

Figure 4. Schematic diagrams of PMD with a) direct contact membrane distillation (DCMD) system, b) air-gap membrane distillation (AGMD) system, and c) vacuum membrane distillation (VMD) system, and d) multi-stage system.

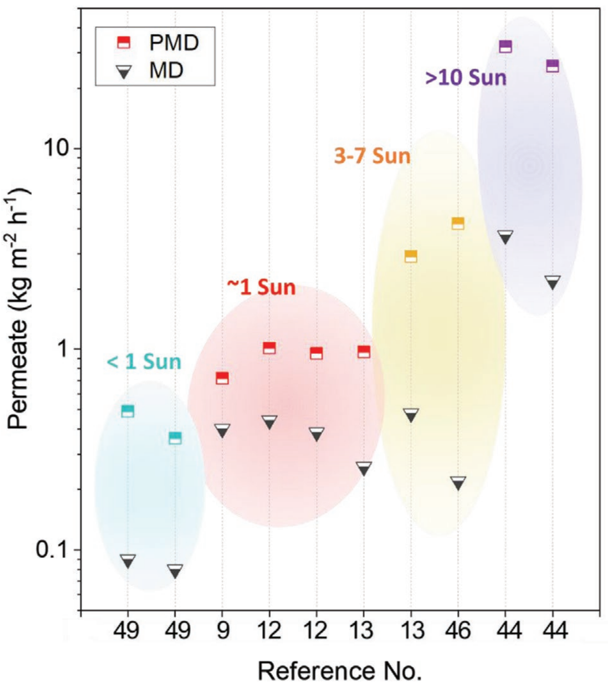

Figure 5. Comparison between the permeate rates of evaporator designs with the photothermal active layer (referred to PMD) and those without (referred to conventional MD) under light irradiation. The comparison was done within the same research group to eliminate other factors that affect the permeate rate, such as device configuration, feed/distillate velocity and temperature, as well as light intensity.[9,12,13,44,46,49]

broadband light absorption, high photothermal conversion efficiency and confined localized heating down to nanoscale. In this section, the design of efficient PMD system in terms of light utilization are considered (**Figure 6**a).

4.1.1. Optical Path

In the first three systems (Figure 4a–c), the photothermal active layer is positioned under the bulk feedwater. The top water layer will greatly attenuate the number of photons absorbed by the photothermal active layer, especially in the case where turbid water is used as the feed.[46] Ho's group[12] has designed the photothermal active layer in a 3D gel form with the feedwater contained inside the 3D gel, and the thickness of the gel was optimized for solar absorption. This is similar to the multi-stage system (Figure 4d) where the photothermal active layer is isolated and directly exposed to sunlight without optical obstruction by the feedwater for maximized light harvesting. Moreover, constructing a hierarchical, hollow or porous structure that favors internal light scattering, minimizes surface light reflection and transmission also helps to improve the solar absorption (Figure 6a).[51–53]

Other than incorporating photothermal materials for light absorption, another advantageous aspect of the photothermal conversion in the active crossflow PMD system lies in light distribution at the evaporation surface. In the conventional MD system, the feed is heated externally and flowed through the module. The highest transmembrane temperature difference is achieved at the feed inlet. As the feed flows across from the inlet to the outlet, the temperature difference reduces due to heat loss. In the PMD system with the same energy input, the entire photothermal active layer absorbs sunlight continuous to engender a high transmembrane temperature difference at the feed outlet (Figure 6b,c).[54] This result has been experimentally demonstrated by Deng's group with the feed temperature increased from 25 to 36.5 °C at the outlet across a 5 cm long device.[13] Moreover, photothermal conversion is independent of the device size in the PMD system, as light is continually supplied throughout the active photothermal layer (Figure 6b). Halas's group[54] verified that increasing the size of the PMD system will increase the overall distillate flux. Unlike in the MD system, the heat loss across the feed channel limits the size of the system and demands a higher feed velocity to compensate the decrease in the temperature gradient across the membrane.

4.1.2. Light Focusing

An alternative approach to manipulate light distribution is through light focusing. Optical concentrators have been used in the conventional solar distillation system to increase the light intensity falling on the evaporation surface. However, focusing optics normally require large footprint and additional infrastructure support. Halas' group[55] took advantage of the exponential temperature dependence of the saturation vapor pressure of water, and designed a PMD system with lens array to redistribute the light on photothermal material (Figure 6d). The lens array focused the light to form small "hot spots" on the photothermal active region that achieved enhanced distilled water flux by more than 50% compared to the lens-less system. Moreover, the footprint remains unchanged as the enhanced distillate flux at the hot spots surpassed the reduction in distillate flux in the other unfocused area of the photothermal active layer (Figure 6e).

4.2. Thermal Management

Thermal management of PMD systems involves enhancing the transmembrane temperature gradient while minimizing the heat loss to the condensation side and the environment. Firstly, directing the heat energy to the targeted location of the system is important in achieving a high permeate rate. Secondly, efficient utilization of the heat flux acquired by photothermal materials in conjunction with superior thermal insulation at the feed-distillate interface, as well as between the device and the environment is essential. These two aspects will be discussed in terms of membrane thermal conductivity and heat allocation in the system.

4.2.1. Thermal Conductivity

The localized heating by the photothermal active layer at the evaporation surface leads to an increase in T_{fs}, and thus the driving force ΔT_s ($\Delta T_s = T_{fs} - T_{ds}$) (Figure 3b). Therefore, heat loss from the feed to the distillate side through conduction

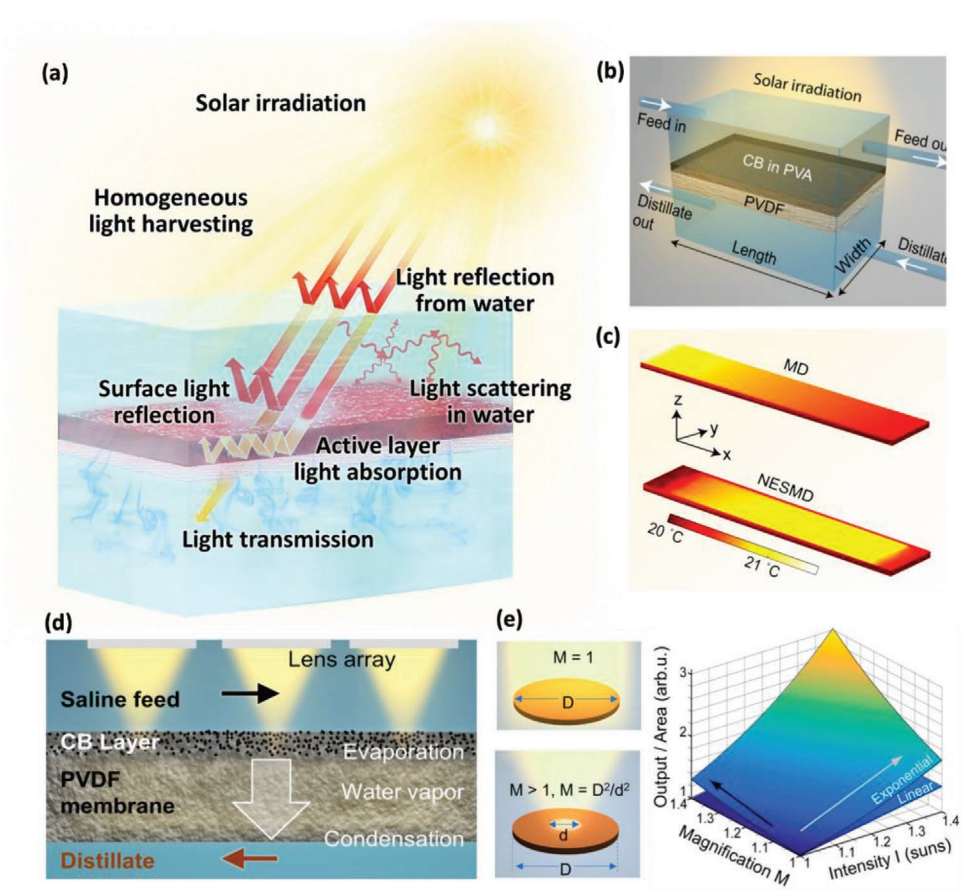

Figure 6. a) Light utilization in PMD system. b) Schematic of the designed nanophotonics-enabled solar MD (NESMD) module.[54] c) Calculated temperature distributions at the membrane surface for MD (top) and NESMD (bottom). The feed inlet temperature is 20 °C in NESMD and 21.3 °C in MD, corresponding to the same input energy in NESMD and MD, with a distillate temperature of 20 °C for both processes.[54] d) Schematic of the cross-section of a solar thermal membrane distillation device under focused illumination.[55] e) Schematic of uniform (left top) and focused (left bottom) illumination on a circular area with diameter *D* and a spot diameter *d*, and the respective output per unit area for linear and exponential processes for different illumination intensities and values of magnification (right).[55] b,c) Reproduced with permission.[54] Copyright 2017, Proceedings of the National Academy of Sciences. d,e) Reproduced with permission.[55] Copyright 2019, Proceedings of the National Academy of Sciences.

should be minimized to further enlarge the ΔT_s. Thermal conductivity of the membrane plays an important role in the heat transfer resistance between the feed and the distillate. In general, the low thermal conductivity of the membrane is required to prevent heat loss to the distillate side, this can be achieved by increasing porosity and thickness of the membrane, or reducing the thermal conductivity of the membrane material.[35] On the other hand, in the case that the photothermal active layer is on top of the hydrophobic membrane, high thermal conductivity of the photothermal active layer is essential for efficient heat transfer to the evaporation surface. Ho's group[12] designed a photothermal catalytic (PTC) gel with orientation-dependent heat transfer ability (**Figure 7**a,b). The anisotropic heat transfer through aligned microchannels exhibits a minimal temperature difference (less than 0.6 °C) between the front and back surface of the PTC gel. The efficient heat transfer through the PTC gel to the evaporation surface displayed high ΔT_s which heightened the overall thermal efficiency of the PMD system. Moreover, introducing a thermal insulation layer can further reduce the temperature polarization effect, thus enhancing thermal efficiency. Cao et al.[56] proposed a hydroxyapatite-chitosan (HA-CS) hybrid film as the insulation layer. The bilayer film reduces the conductive heat dissipation across the membrane and remarkably impairs the temperature polarization. In the presence of the thermal insulation layer, larger ΔT_s (= $T_4 - T_3$) is preserved (Figure 7c), leading to higher solar efficiency of 61% compared with sole photothermal layer (43%) under 1 sun illumination.

4.2.2. Heat Allocation

Another factor that affects the heat transfer and the temperature polarization in the active crossflow PMD system is the feed flowrate (Figure 7d). In the conventional MD system, the permeate flux increases with the feed flowrate, as a result of reduced temperature polarization effect and fast exchange of lower temperature feed near the outlet. In contrast, the PMD system is more efficient with lower feed flowrate which allows more time for light irradiation to increase the transmembrane temperature gradient.[54] This trend has been studied by various groups. Jun's group evaluated the influence of the flowrate on the PMD system by increasing the feed flowrate from 1.5 to 8.1 mL min^{-1},

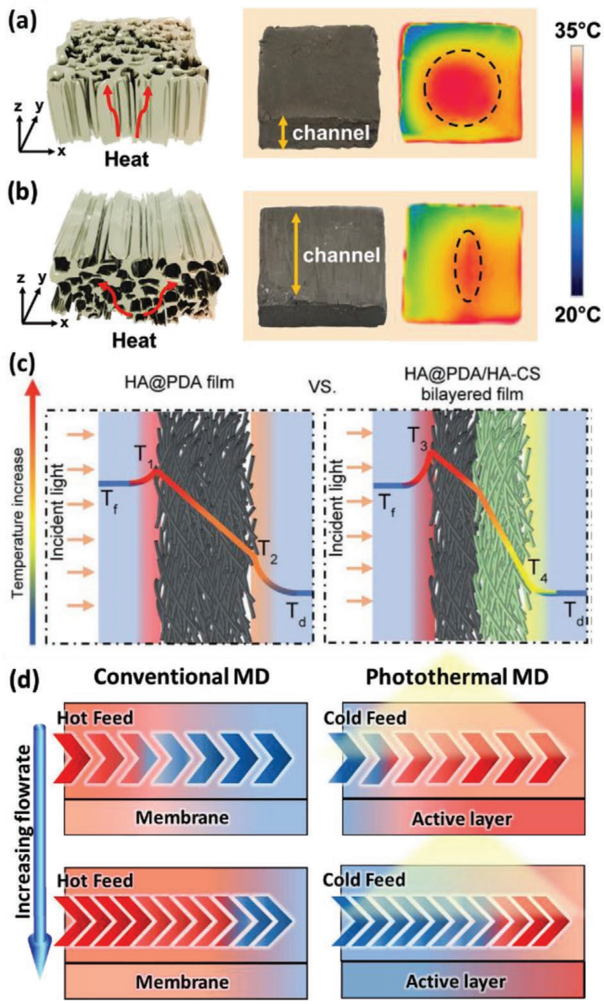

Figure 7. Schematic representations of heat conduction through the PTC gel with heat supplied at the bottom, and the digital photos and infrared images in the vertical orientation a) and the horizontal orientation b) respectively.[12] c) Schematic illustration of the thermal profile using polydopamine-coated hydroxyapatite nanowires (HA@PDA) as the photothermal active layer, with (right) and without (left) thermal insulation layer (HA-CS) under solar irradiation.[56] d) Schematic diagram of the temperature changes in MD and PMD systems with increasing feed flowrates. Red indicates high temperature and blue indicates low temperature. a,b) Reproduced with permission.[12] Copyright 2020, Wiley-VCH GmbH. c) Reproduced with permission.[56] Copyright 2020, Royal Society of Chemistry.

the permeate rate with both pure and saline water decreased from 0.66 to 0.49 kg m^{-2} h^{-1}, and from 0.57 to 0.43 kg m^{-2} h^{-1}, respectively.[46] Wang's group also observed a similar trend with the flowrate varied from 5, 6 to 7 g h^{-1}, the permeate rate decreased to 1.93, 1.83, and 1.76 kg m^{-2} h^{-1}, respectively. While in the case with no water flowing out of the device, the permeate rate was maximized at 2.09 kg m^{-2} h^{-1}.[32] The PMD system benefits from low flowrate, and more so with dead-end water, which further reduces the energy required for water circulation and boosts the overall energy efficiency. In addition, this is also an added advantage that allows the PMD system to be operated at off-grid locations with poor access to electricity.

The performance of the PMD is also affected by the heat exchange with the environment. When the device is operating at a higher temperature than the environmental temperature, heat will be lost through radiation and convection. Halas's[54] group studied the effect of ambient temperature on the permeate rate of PMD system with the feed and the distillate operating at 20 °C. The results show more than two times improvement with the ambient temperature increased from 10 to 40 °C. Their results also revealed that the system with larger-dimension benefits more with higher ambient temperature. Other researchers have demonstrated the utilization of ambient energy harvesting to improve the evaporation rate of their solar absorbers.[52,57–62] The lower surface temperature of the solar absorber not only allows the net gain of energy from the environment, but also reduces heat loss to the environment. Efforts have also been done to reduce the heat loss to ambient by insulating the system. The device designed by Wang's group[14] sealed the sides of the device with polyurethane foam. With negligible heat loss through the side surface, the efficiency is increased by ≈40% compared with the non-insulated device. Moreover, a layer of optically transparent (>95%) silica aerogel was used for thermal insulation above the photothermal active layer to suppress heat losses.[14] The insulation for the top layer in the isolation configuration needs to be carefully chosen as it mandates high light transmittance to avoid compromised light absorption by the photothermal active layer.

4.3. Condenser Design

The last process of the PMD system is condensation. The large transmembrane temperature gradient provides high vapor diffusion across the membrane. The condensation side should not hinder the diffusion while providing effective cooling for distillate collection. Moreover, the energy required for thermal distillation is rather high (≈2400 kJ kg^{-1}) due to the transferred latent heat of vaporization.[35] Recovery of the latent heat from vapor condensation is therefore critical to go beyond the 100% thermodynamic theoretical limit of solar-to-vapor conversion efficiency. Various configurations (Figure 4) have been developed and their differences are discussed in the section.

4.3.1. Direct Contact and Air-Gap Systems

Facilitating latent heat recovery plays a key role in enhancing thermal distillation efficiency. The commonly discussed configuration adopted from conventional MD is the direct contact membrane distillation (DCMD) system which uses two separate streams for the feed and the distillate.[45,48,54,63] This is mainly due to the simple module design that allows the researchers to explore the influence of various factors on PMD system. In this system, latent heat recovery can be realized by an external heat exchanger that transfers heat from the distillate back to the feed (Figure 4a), leading to substantially reduced energy input by more than an order of magnitude.[64] Further improvements in energy efficiency can be achieved by air-gap membrane distillation (AGMD) configuration which the cold stream for cooling can be directly used as feed after collecting the latent heat (Figure 4b).[65,66] In this case, a separate distillate stream is not required at the beginning of the operation, and latent heat recovery can be realized without external heat exchanger, thus allowing simplified operation and more compact design.[35]

4.3.2. Vacuum System

Vacuum membrane distillation (VMD) has also been used for PMD which permits higher partial pressure gradient with less conductive heat loss, thus derives higher permeate flux compared with DCMD and AGMD system.[10,44] Curcio's group[44] developed silver nanoparticle-loaded PVDF membrane for PMD adopting VMD configuration, results in 11-fold higher permeate flux than the pure PVDF membrane under UV irradiation. However, this configuration demands a high standard for the mechanical strength of the membrane layer and the adhesion stability of the loaded photothermal materials since the vacuum condition creates a high absolute pressure difference across the membrane.[67] In addition, heat recovery is technically difficult to be implemented due to the complicated setup associated with vacuum and external condensers (Figure 4c).[68]

4.3.3. Multi-Stage System

To utilize heat more efficiently, novel PMD modules with multi-stage latent heat recovery systems were designed based on DCMD and AGMD distillate collection systems (Figure 4d). The heat released through the condensation process is used to preheat the feed stream for the next stage evaporation. The feed and distillate separation can be accomplished either using a hydrophobic membrane (Figure 4d-i) or with a small air gap in the passive system (Figure 4d-ii). Moreover, the isolation of the photothermal active material from the bulk water eliminates light interference from the top water level. Chiavazz et al.[31] presented their passive solar distiller with commercial spectral selective solar absorber in a multi-stage system. Feedwater supply to the system relies on capillary forces, while distillate collection is based on gravity. Natural convection is used for cooling through the aluminum heat sink at the last stage. With this passive design, the three- and ten-stage devices showed a 3- and 6-fold enhancement compared with the single-stage distiller. This translates to a solar-to-distillate efficiency beyond 200% under one sun irradiation. Wang et al.[32] adopted a similar design with photovoltaic panel as the photothermal active layer in a three-stage device and demonstrated ≈139% solar-to-water conversion efficiency. The recent work by Xu et al.[14] using a ten-stage air-gap configuration device, reported a record-high conversion efficiency of 385% and GOR larger than four. The high efficiency was achieved with optimized device geometry, the number of stages and sidewall thermal insulation.

In general, the PMD system overcomes the intrinsic limitations of conventional MD including low thermal efficiency, high energy consumption and lack of scalability. The localized heating at the evaporation surface inverses the temperature polarization effect, and also minimizes heat loss to both the bulk feed and the environment, thus largely improves the thermal efficiency of the system. Besides, the solar-enhanced transmembrane temperature gradient favors slow flowrate, thus reduced electrical energy for feedwater circulation and preheating. Moreover, high thermal resistance of the membrane, better insulation of the system and the latent heat recovery design further reduce the heat loss. In addition, the permeate rate increases with membrane module size in the PMD system, making this system scalable.[10] Conversely, the passive design with hydrophilic wicking materials for water supply is suitable for small-scale and low-cost water production systems.

5. Photothermal Active Layer Design Considerations

Photothermal nanomaterials, owing to their unique electronic and optical properties, display localized heating under solar irradiation. Coupled with large surface area, tunable surface properties, and controllable structures, they are favorable to be incorporated into PMD system. Currently, the most commonly used hydrophobic membranes in MD are poly(vinylidene-fluoride) (PVDF), poly(tetrafluoroethylene) (PTFE), and poly(propylene) (PP).[45] In this section, photothermal materials innovation and various material incorporation configurations with the membrane distillation will be compared and discussed.

5.1. Photothermal Materials Innovation

Carbon-based materials, plasmonic nanoparticles, semiconductors and macromolecules with narrow bands have been demonstrated for efficient photothermal conversion, with materials innovation typically based on their different mechanisms, namely thermal vibration, localized surface plasmon resonance, and optical excitation-nonradiative relaxation, respectively.[39,47,55,69,70] Carbon-based materials with the advantage of full solar spectrum absorption have been adopted as photothermal materials extensively,[47] such as carbon nanotubes, graphene, carbon black, biomass or natural products derived carbon materials.[3,71–81] Current strategies in preparing carbon-based solar absorbers generally focus on minimizing surface light reflection through structure design. Plasmonic nanomaterials (e.g., Au, Ag, Al) with high photothermal conversion efficiency have also been used in solar evaporation, however, they normally exhibited narrowband plasmonic resonances. To manipulate or broaden the light absorption range involves tuning the particle size, geometry, composition, intra/interparticle distance and dielectric environment.[18,19,82–84] Semiconductors, such as metal oxides and chalcogenides are promising photothermal materials due to the tunability in their absorption range and large extinction coefficients in the NIR region.[47,85] Their optical properties can be modified through bandgap engineering by introducing donor/acceptor sites and mid-gap electronic states.[86] Moreover, the LSPR effect in semiconductors enhances the photothermal conversion efficiency due to higher probability of nonradiative recombination in the presence of excess free carriers.[87–89] Other materials, such as MXene, organic polymer and ceramics have also been used for photothermal vaporization.[2,27,90–92] In addition, researchers claimed that the nanostructured molecular

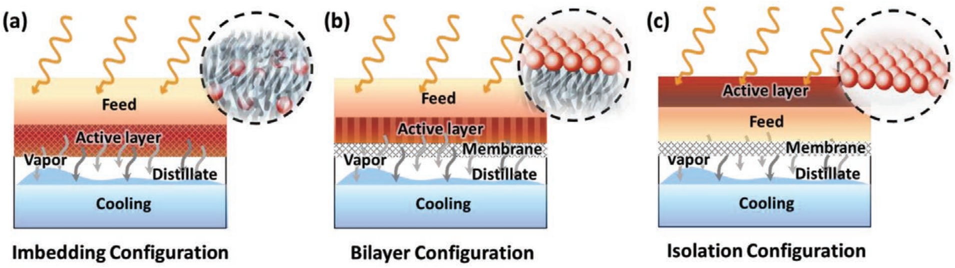

Figure 8. Schematic diagrams of a) imbedding configuration with photothermal materials embedded in the membrane, b) bilayer configuration with photothermal active layer positioned on top of the membrane, and c) isolation configuration with the photothermal active layer separated from the membrane, illustrating using air-gap system.

hydrogel meshes enables water evaporation as clusters instead of individual molecules and thus reduces the water latent heat leading to high production rate[27,93,94]

The photothermal materials used in PMD system are similar to the solar absorbers in solar steam generation. Various photothermal materials incorporated into membrane distillation have been demonstrated, including carbon black,[10,54,55] graphene,[9] plasmonic particles,[44,95] MXene,[63] polymers,[11,46,56] semiconductor Fe_3O_4,[13] composite materials such as Pt–Ag Ni foam[96] and chitosan gel with TiO_2/Ag fiber.[12] Other than these, commercial materials have also been applied in isolation systems, such as TiNOX,[31] and PV panel.[32]

5.2. Configurations of Photothermal Material Incorporation

Besides its photothermal properties, the design of the photothermal active layer requires other pertinent characteristics, such as high porosity for vapor diffusion, hydrophobic surface for feed-distillate separation, mechanical and chemical stability. All these properties are related to the incorporation methods. To date, various methods have been undertaken to incorporate the photothermal materials into the membrane system, such as pre-mixing the photothermal materials with scaffolds or polymer powder followed by membrane casting[44] or electrospinning[54,95] binder adhesive[10] or direct coating on membrane through vacuum filtration,[9,13,56,63] spraying,[48] gas phase deposition,[45] and chemical growth.[96] Others developed isolated photothermal active layer,[11,12] or directly adopting commercial spectrally selective solar absorber.[14,31] Based on different incorporation methods, we classified them into three different configurations. The first shows the imbedding configuration where the photothermal materials are mixed into the membrane (**Figure 8**a), the second is the bilayer configuration with photothermal active layer loaded or positioned on top of the membrane (Figure 8b). The last is the isolation configuration with the photothermal active layer separated from the membrane (Figure 8c). The differences in various designs in terms of photothermal properties, wettability, permeability and durability will be discussed (**Figure 9**).

5.3. Photothermal Properties

High solar absorption of the photothermal active layer is the foundation for an efficient PMD system (Figure 9a). Improving its light harvesting can be done through material design and optical path manipulation as discussed previously. Other than that, the quantity or thickness of the materials will greatly affect its light-harvesting capability based on penetration depth, thus the efficiency of photothermal conversion. The amount of photothermal nanomaterials used directly affects the transmembrane temperature difference. Curcio's group[44] studied the effect of Ag nanoparticles loading amount on the PVDF membrane. As the percentage of loading increased from 15 to 25 wt%, the interface temperature raised by ≈10 K, which results in transmembrane flux of 4-fold increment. It is worth noting that the loading amount will also affect the mass transfer of the generated vapor as both the thermal conductivity and the porosity of the membrane in the imbedding and bilayer systems will be modified.

In terms of transmembrane heat loss (Figure 9b), bilayer configuration (Figure 8b) may offer a better cross-membrane thermal insulation due to the extra membrane layer with relatively high thermal resistance, thus reduced heat loss to the condenser. In the isolation configuration (Figure 8c), heat

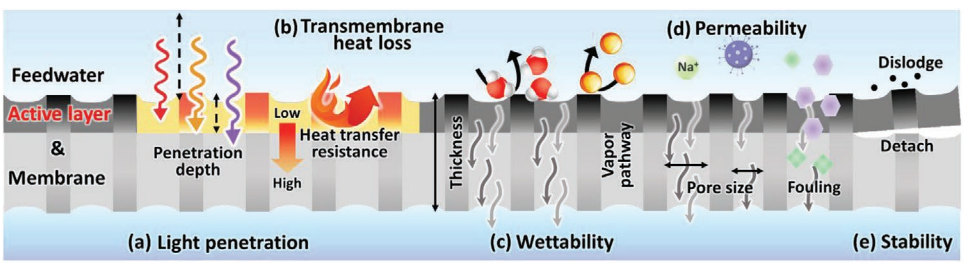

Figure 9. Schematic diagram of various properties of the photothermal active layer and membrane in PMD.

is transferred to the evaporation surface through the feed. In order to improve the thermal efficiency of the isolation configuration, researchers have adopted hydrophilic sheet/foam to constrict a thin layer of feedwater through wicking or pumping, thus reduced the conduction loss from the photothermal active layer to the evaporation surface.[11,32]

5.4. Wettability

In order to maintain long-term operation stability, the membrane surface should be hydrophobic to resist liquid penetration but allow water vapor to pass through (Figure 9c). In the imbedding configuration, surface hydrophobic modification is normally required to retain the water separation,[56] while in the bilayer and isolation configurations, the hydrophobic membrane performs this function. Although the PMD system can reject non-volatile solutes, such as macromolecules, colloids and ions, the commonly used commercial hydrophobic membrane cannot repel low-surface-tension contaminants (e.g., mineral oil and ethanol). These contaminants in the feed will infiltrate the membrane pores and cause surface pore wetting and fouling, thus reducing the lifetime of the membrane (Figure 9d).[97,98] To solve this problem, much research has been devoted to develop omniphobic membrane with extremely low surface energy of the membrane surface that repels the low-surface-tension contaminants.[99] Gong et al.[48] engineered a multilevel-roughness membrane that allows effective control of surface wettability. The excellent anti-fouling and anti-wetting properties lead to a stable permeate rate over 48 h when operating in oil-contaminated and high-salinity solution, which significantly outperforms the commercial distillation membranes. Additionally, in the case when capillary force is used to drive the feed to the evaporation surface, hydrophilic properties are required for sufficient water supply. Water-absorbing materials, such as cellulose fibers,[14] polyvinyl alcohol sponge,[11] and quartz glass fibrous membrane[32] have been used as the feed layer for water wicking purpose.

5.5. Permeability

Other than the driving force of thermal energy, the intrinsic properties of the photothermal active layer and the membrane will also affect the vapor permeability across the membrane, such as porosity and thickness. Increasing porosity and thickness of the membrane will increase the thermal resistance of the membrane, beneficial for high transmembrane temperature gradient. However, this may hinder the vapor transport across the membrane. Moreover, direct addition of binders, or photothermal materials onto the membrane also inevitably decreases the pores and thus reduces the vapor permeability (Figure 9d).[96] In the bilayer configuration, various porous structures are adopted to facilitate both water transport and vapor permeation, including microporous superstructure,[48] binder-free porous network,[96] and 3D gel with aligned pores.[12] It is worthwhile to mention that in the system with air-gap design, minimizing membrane thickness is always favorable as the air-gap width is usually 10–100 times greater than the membrane thickness.[100] In this case, the larger air-gap guarantees a higher transmembrane temperature gradient due to lower thermal transmittance of air, however reduces the permeability coefficient. Thus, heat and mass transfer properties need to be fine-tuned in the air-gap design.[31]

In addition, membrane fouling leads to reduction in the membrane permeability coefficient and thermal resistance, thus decreasing solar-to-distillate efficiency (Figure 9d).[101] MD is generally considered to have a lower fouling propensity due to large membrane pore size and low operating pressure as compared with high pressure-driven membrane technologies such as reverse osmosis and nanofiltration.[102] Moreover, study has shown the lower operating temperature in PMD increases the solubility of common scalants and decreases salt precipitation rates as that observed in conventional MD. Scaling can be reduced by providing localized surface heating at them membrane, instead of bulk water heating, to drive permeation in PMD.[103] Nevertheless, in the passive PMD system where dead-end water or wicking are applied, salt accumulation may occur in the photothermal active layer or the hydrophilic layer. This high salinity reduces the permeate flux (refer to Equation (2)). The passive salt removal process which involves diffusion of the high-salinity water in the hydrophilic layer back into the source due to the concentration gradient can be executed during night-time. However, this process is rather slow and the time available for salt removal may not be enough especially in the large-scale modules. Asinari's group[31] used an additional flow of seawater in a rinse basin connected to the hydrophilic layers for efficient rinsing of the salt accumulated in the hydrophilic layers at night (**Figure 10**).

5.6. Durability

The durability of the active photothermal layer should be deliberated, especially in the first two systems where it is positioned beneath the water. The current design may face issues associated to membrane fragility, dislodgement of nanomaterials, or detachment of the active layer from the membrane (Figure 9e), thus affecting the lifetime and recyclability.[44] This may also limit the flowrate of the feed to avoid nanomaterials shearing. Although the PMD system operates better under stagnant water conditions, the combination with additional low-grade heat input for feedwater in the continuous flow system favors a high flowrate. Ang et al.[96] demonstrated directly grown plasmonic nanostructures on nickel foam that withstood high flowrate. The results showed improved permeate flux from ≈3.7 to ≈8 kg m^{-2} h^{-1} with light irradiation under the flowrate of 250 and 2000 mL min^{-1}, respectively. Further improvements on the robustness and adhesion of the photothermal active layer are required for high durability in practical applications for the treatment of challenging feedwater.

6. Photothermal Membrane Distillation Applications

To date, most conventional water purification technologies are usually accompanied by high energy consumption and large

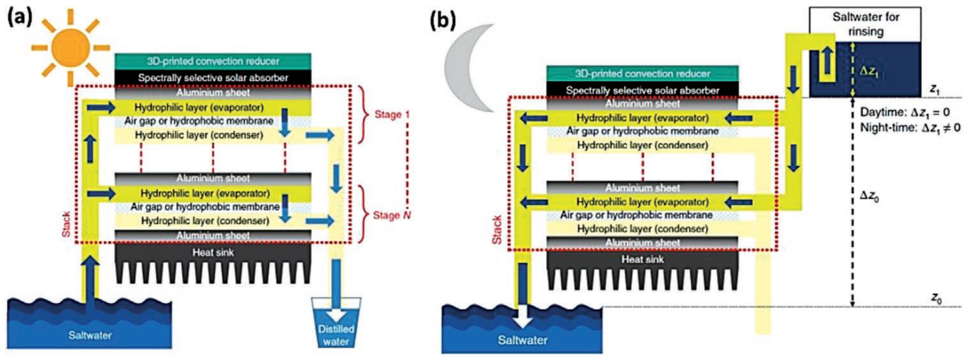

Figure 10. Schematic of the modular distiller during a) daytime desalination operation and b) night-time salt removal process.[31] Reproduced with permission.[31] Copyright 2018, Springer Nature.

centralized infrastructure. The advancement made in photothermal materials, which can effectively harvest abundant solar energy, largely improved the efficiency of solar distillation. Incorporating photothermal materials into membrane distillation becomes an attractive approach for freshwater production with enhanced thermal efficiency and reduced electricity input. PMD system has the capability to obtain pure water from desalination, close to 100% salt rejection rate. It is commended for the ability to treat high-salinity brines which cannot be administered by reverse osmosis.[35] Moreover, other solar-driven technologies can be strategically integrated with the PMD system to achieve synergetic multi-functions with enhanced solar utilization. In this section, we will explore the practical applications of this technology toward desalination, water purification, and energy generation.

6.1. Desalination

In direct solar desalination process, the low efficiency due to poor solar absorption of the seawater and massive heat loss limit its practical applications. With the integration of photothermal materials into the PMD system, the solar-to-distillate conversion efficiency has been greatly improved. This opens a possibility for household freshwater production with modular desalination device under natural sunlight, given that the average daily water intake is ≈3.2 L for one adult.[104] Various device configurations have been designed and demonstrated under outdoor conditions.

Several approaches have been used to enhance the thermal efficiency under natural sunlight. Halas's group[54] utilized Fresnel lens to concentrate the solar light by 25 times, and realized significantly higher photothermal distillate flux of 5.2 kg m^{-2} h^{-1} compared to unfocused case (0.22 kg m^{-2} h^{-1}) (**Figure 11**a). The salt rejection rate is >99.5% with photothermal active layer in this direct contact PMD system. Said et al.[10] used a solar panel to provide electric power for pumping the water and air to the reactor in their vacuum PMD system (Figure 11b). They achieved an average permeate flux of 0.55 kg m^{-2} h^{-1} and a salt removal rate of 99.8% under solar irradiation intensities ranging between 88 and 1012 W m^{-2}. The multi-stage system with latent heat recovery is able to achieve distillate production rate above the thermodynamic limit of single-stage solar still. Chiavazzo et al.[31] have tested their passive distiller for desalination for rooftop (Figure 11c) and sea (Figure 11d) settings, with natural cooling using heat sink and seawater, respectively. The 3-stages distiller achieved permeate production of 0.585 on the rooftop and 1.5 kg m^{-2} h^{-1} in the sea

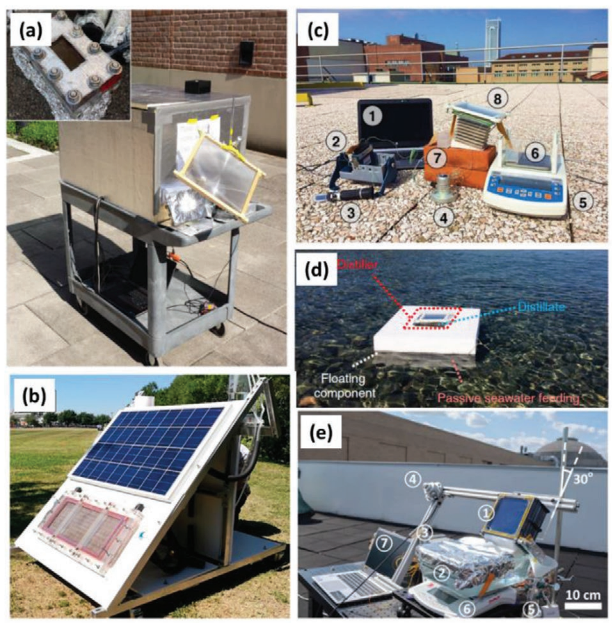

Figure 11. a) System setup on a cart with all components except the module (inset), Fresnel lens, power meter, and computer enclosed inside.[54] b) Front view of the system with PMD at the bottom and solar panel for pumping water/air on the top.[10] c) Outdoor roof-top testing of the modular distiller with 1) a laptop for data storage and elaboration, 2) a data acquisition board, 3) an analogic refractometer for salinity measurement, 4) a pyranometer for solar irradiance measurement, 5) a scale for distillate mass measurement, 6) an output basin for the distilled water, 7) an input basin for the saltwater, and 8) the modular distiller.[31] d) Floating installation of the modular distiller.[31] e) Experimental setup with the ten-stage prototype on a partly sunny day with scattered clouds on a rooftop, consisted of 1) a ten-stage TMSS device, 2) a water reservoir, 3) an aluminum extrusion frame, 4) a pyranometer, 5) 100 mL graduated cylinder, 6) a balance, and 7) a computer.[14] a) Reproduced with permission.[54] Copyright 2017, Proceedings of the National Academy of Sciences. b) Reproduced with permission.[10] Copyright 2019, American Chemical Society. c,d) Reproduced with permission.[31] Copyright 2018, Springer Nature. e) Reproduced with permission.[14] Copyright 2020, Royal Society of Chemistry.

under solar irradiance at ≈600 and ≈846 W m^{-2}, respectively. The 10-stages distiller achieved permeate production of 1.32 kg m^{-2} h^{-1} on the rooftop setting. Wang's group[14] also tested the passive 10-stage prototype with optimized heat and mass transfer design under outdoor environments, where the prototype was fixed on a frame with 30° tilt (Figure 11e). On a cloudy day with solar irradiation fluctuates between 200 to 800 W m^{-2}, a total of 72 mL of water was collected within 4.5 h. With 100 modular devices of 1 m^2, it could provide ≈10–20 L of clean water daily depending on the weather condition.

6.2. Multifunctional Applications

Solar energy has been widely used for clean energy generation through photovoltaic, photochemical, and photothermal processes. The strategic photothermal distillation integration with energy generation is a logical solution for sustainable development in relation to the water-energy nexus.[3,105–112] Emerging research on PMD system with correlated solar-driven applications for parallel freshwater production and energy generation is becoming more evident.

Ho's group[12] developed a H_2O–H_2 co-generation system (HCS) that enables concurrent freshwater and clean energy output with a PTC gel in PMD system (**Figure 12**a). Upon solar irradiation, the PCT gel will generate vapor and photocatalytic hydrogen simultaneously. Both the vapor and H_2 gas will pass through a hydrophobic membrane, where distillate and hydrogen are collected from the respective bottom and top outlet of the collector (Figure 12b). The PTC gel exploits localized plasmonic heating at the nanoscale level and confined thermal heating at the macroscopic level, which facilitates synergetic enhancement in both photocatalytic hydrogen generation and solar desalination processes. The HCS demonstrated photothermal-enhanced daily freshwater production of 5000 g m^{-2} and hydrogen production of 4600 µmol m^{-2} under natural sunlight (Figure 12c). This system manifests the advantages of low-grade solar heat utilization and high-salinity brine operation to provide an environmentally attractive and sustainable solution for desalination and energy generation.

Another work done by Wang's group[32] demonstrated a photovoltaics-membrane distillation (PV-MD) device where PV panel is employed as both photovoltaic component for electricity generation and photothermal component for clean water production (Figure 12d). The multi-stage membrane distillation device is attached to the backside of PV, waste heat generated from PV will be directly used to drive the water distillation process with latent heat recovery. The electricity generation efficiency of the PV panel was not compromised by the MD device. The hybrid design produced clean water of 1.64 kg m^{-2} h^{-1} and electricity generation of ≈11% under one sun irradiation (Figure 12e,f). This strategy does not only reduce the capital investment costs by sharing the footprint and mooting system, but also provide a possibility to transform an electricity generation plant water consumer to a freshwater producer.

7. Conclusions and Perspective

In summary, we have presented a comprehensive review of the recent progress in photothermal membrane distillation. Firstly,

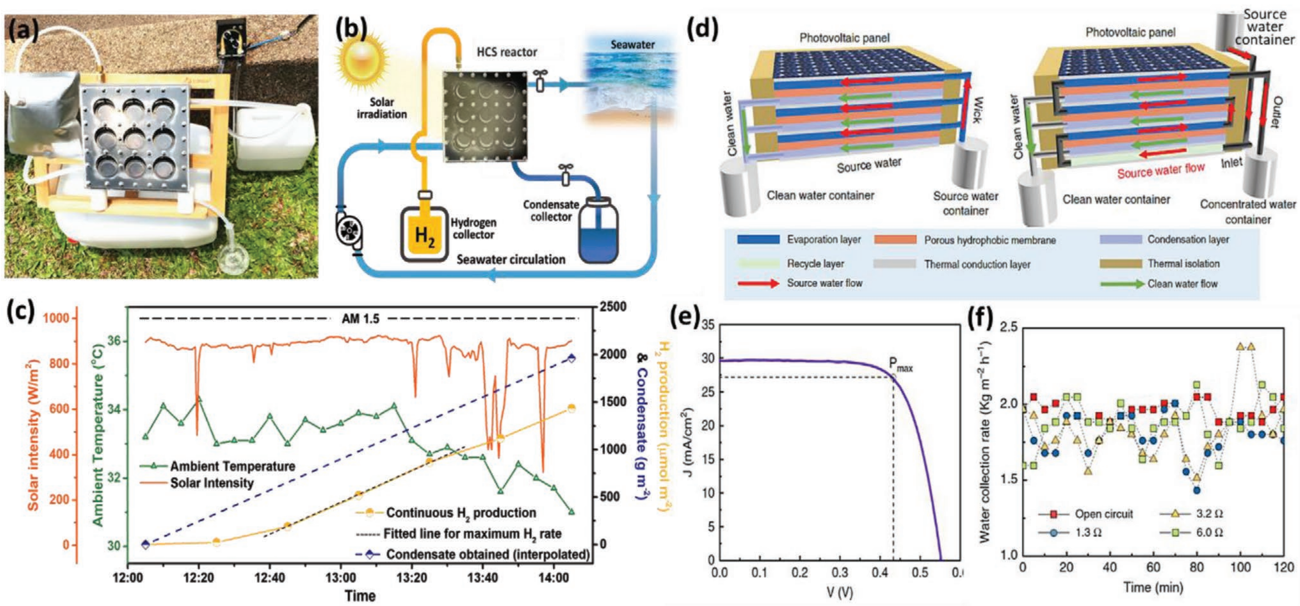

Figure 12. a) Digital photo of the H_2O–H_2 co-generation system (HCS) for outdoor testing. b) Schematic diagram and c) the measured results of the H_2O–H_2 co-generation prototype for concurrent photocatalysis and desalination of seawater under natural sunlight.[12] d) Schematic illustration of the integrated photovoltaics-membrane distillation (PV-MD) devices with dead-end and cross-flow modes. e) *J*–*V* curve of the solar cell under one sun illumination (P_{max} refers to the maximum power). f) Clean water production rate at different loads of three-stage PV-MD with dead-end mode.[32] a–c) Reproduced with permission.[12] Copyright 2020, Wiley-VCH GmbH. d–f) Reproduced with permission.[32] Copyright 2019, Springer Nature.

the fundamental mechanism of photothermal conversion and membrane distillation are covered. Secondly, various strategies have been examined for designing efficient PMD system from photothermal conversion to vaporization and condensation process. Different aspects including material manipulation for light harvesting and localized heating, light and heat distribution in PMD system, condenser design with various configurations concerning latent heat recovery system, are presented. Thirdly, various methods for incorporating the photothermal active layer into the membrane are introduced. The criterial of various designs in terms of photothermal properties, wettability, permeability, and durability are discussed. Lastly, applications of PMD system in desalination and water treatment, as well as integrating with other solar-driven technologies for freshwater production and energy generation have been reviewed.

The integration of photothermal materials into an existing thermal membrane desalination technology largely enhances the thermal efficiency of MD process through photothermal localized heating. Meanwhile, it resolves the lack of efficient clean water collection systems in the current solar steam generation field. This novel PMD technology enables easy distillate collection through direct contact, air-gap or vacuum system configurations. Moreover, PMD can operate at low pressure, making it suitable for treating high salinity water with high salt rejection rate and diminished fouling problems, thus minimizes the salt accumulation issues which can potentially occur in solar steam generation. Furthermore, in terms of energy consumption, PMD mainly operates using the abundant and sustainable solar energy at low temperature and low pressure,[95] thereby it is less energy-intensive compares to conventional MD and reverse osmosis processes.[21] Therefore, it is a promising technique with relatively simple infrastructure for small-scale clean water generation in the remote off-grid regions.

The photothermal materials used in PMD system is similar to the solar absorbers in solar steam generation, with desirable properties like broadband solar absorption, multiple light scattering and trapping, and high photothermal conversion efficiency. However, the design of the photothermal active layer requires other pertinent characteristics, such as high porosity for vapor diffusion, hydrophobic surface for feed-distillate separation, mechanical and chemical stability. Therefore, more efforts are needed to develop highly durable photothermal materials with relevant features for integrating into the membrane systems. Moreover, fundamental understanding of heat and mass transport in the PMD system are crucial for high-performance device design. The scalability of PMD system with efficient latent heat recovery, minimized heat loss and compact design still need to be investigated. Besides, demonstration of PMD system combined with low-grade heat energy sources, such as industrial waste heat, can be further explored to improve the overall efficiency of the system. In addition, PMD not only empowers freshwater production from desalination, but also can be potentially integrated with other collegial applications in the areas of polluted/contaminated water treatment and energy generation. Finally, the economic and ecological benefits of the PMD system have to be carefully accessed before the technology can be widely adopted for providing safe and affordable water supply.

Acknowledgements

This research was supported by A*STAR under its 2019 AME IRG & YIRG Grant Calls, A2083c0059.

Conflict of Interest

The authors declare no conflict of interest.

Keywords

desalination, freshwater production, nanomaterial membranes, photothermal distillation, solar evaporation

Received: December 1, 2020
Revised: January 27, 2021
Published online: February 15, 2021

[1] UNESCO, UN-Water, *United Nations World Water Development Report 2020: Water and Climate Change*, UNESCO, 7, Place de Fontenoy, 75352 Paris 07 SP, France **2020**.
[2] L. Zhang, B. Tang, J. Wu, R. Li, P. Wang, *Adv. Mater.* **2015**, *27*, 4889.
[3] L. Zhu, M. Gao, C. K. N. Peh, X. Wang, G. W. Ho, *Adv. Energy Mater.* **2018**, *8*, 1702149.
[4] Q. Yang, C. Xu, F. Wang, Z. Ling, Z. Zhang, X. Fang, *ACS Appl. Energy Mater.* **2019**, *2*, 7223.
[5] B. Gong, H. Yang, S. Wu, G. Xiong, J. Yan, K. Cen, Z. Bo, K. Ostrikov, *Nano-Micro Lett.* **2019**, *11*, 51.
[6] Y. Zhang, S. K. Ravi, L. Yang, J. V. Vaghasiya, L. Suresh, I. Tan, S. C. Tan, *ACS Appl. Mater. Interfaces* **2019**, *11*, 38674.
[7] L. Cui, P. Zhang, Y. Xiao, Y. Liang, H. Liang, Z. Cheng, L. Qu, *Adv. Mater.* **2018**, *30*, 1706805.
[8] G. Ni, S. H. Zandavi, S. M. Javid, S. V. Boriskina, T. A. Cooper, G. Chen, *Energy Environ. Sci.* **2018**, *11*, 1510.
[9] L. Huang, J. Pei, H. Jiang, X. Hu, *Desalination* **2018**, *442*, 1.
[10] I. A. Said, S. Wang, Q. Li, *Ind. Eng. Chem. Res.* **2019**, *58*, 18829.
[11] G. Xue, Q. Chen, S. Lin, J. Duan, P. Yang, K. Liu, J. Li, J. Zhou, *Global Challenges* **2018**, *2*, 1800001.
[12] M. Gao, C. K. Peh, L. Zhu, G. Yilmaz, G. W. Ho, *Adv. Energy Mater.* **2020**, *10*, 2000925.
[13] W. Li, Y. Chen, L. Yao, X. Ren, Y. Li, L. Deng, *Desalination* **2020**, *478*, 114288.
[14] Z. Xu, L. Zhang, L. Zhao, B. Li, B. Bhatia, C. Wang, K. L. Wilke, Y. Song, O. Labban, J. H. Lienhard, R. Wang, E. N. Wang, *Energy Environ. Sci.* **2020**, *13*, 830.
[15] T. A. Cooper, S. H. Zandavi, G. W. Ni, Y. Tsurimaki, Y. Huang, S. V. Boriskina, G. Chen, *Nat. Commun.* **2018**, *9*, 5086.
[16] W. Li, Z. Li, K. Bertelsmann, D. E. Fan, *Adv. Mater.* **2019**, *31*, 1900720.
[17] H. Ghasemi, G. Ni, A. M. Marconnet, J. Loomis, S. Yerci, N. Miljkovic, G. Chen, *Nat. Commun.* **2014**, *5*, 4449.
[18] L. Zhou, Y. Tan, J. Wang, W. Xu, Y. Yuan, W. Cai, S. Zhu, J. Zhu, *Nat. Photonics* **2016**, *10*, 393.
[19] L. Zhou, Y. Tan, D. Ji, B. Zhu, P. Zhang, J. Xu, Q. Gan, Z. Yu, J. Zhu, *Sci. Adv.* **2016**, *2*, e1501227.
[20] P. Tao, G. Ni, C. Song, W. Shang, J. Wu, J. Zhu, G. Chen, T. Deng, *Nat. Energy* **2018**, *3*, 1031.
[21] S. Cao, Q. Jiang, X. Wu, D. Ghim, H. Gholami Derami, P.-I. Chou, Y.-S. Jun, S. Singamaneni, *J. Mater. Chem. A* **2019**, *7*, 24092.
[22] S. K. Patel, C. L. Ritt, A. Deshmukh, Z. Wang, M. Qin, R. Epsztein, M. Elimelech, *Energy Environ. Sci.* **2020**, *13*, 1694.

[23] C. Chen, Y. Kuang, L. Hu, *Joule* **2019**, *3*, 683.
[24] F. Zhao, Y. Guo, X. Zhou, W. Shi, G. Yu, *Nat. Rev. Mater.* **2020**, *5*, 388.
[25] X. Wu, L. Wu, J. Tan, G. Y. Chen, G. Owens, H. Xu, *J. Mater. Chem. A* **2018**, *6*, 12267.
[26] Y. Yang, R. Zhao, T. Zhang, K. Zhao, P. Xiao, Y. Ma, P. M. Ajayan, G. Shi, Y. Chen, *ACS Nano* **2018**, *12*, 829.
[27] F. Zhao, X. Zhou, Y. Shi, X. Qian, M. Alexander, X. Zhao, S. Mendez, R. Yang, L. Qu, G. Yu, *Nat. Nanotechnol.* **2018**, *13*, 489.
[28] Y. Yang, X. Yang, L. Fu, M. Zou, A. Cao, Y. Du, Q. Yuan, C.-H. Yan, *ACS Energy Lett.* **2018**, *3*, 1165.
[29] K. H. Nayi, K. V. Modi, *Renewable Sustainable Energy Rev.* **2018**, *81*, 136.
[30] P. J. J. Alvarez, C. K. Chan, M. Elimelech, N. J. Halas, D. Villagrán, *Nat. Nanotechnol.* **2018**, *13*, 634.
[31] E. Chiavazzo, M. Morciano, F. Viglino, M. Fasano, P. Asinari, *Nat. Sustain.* **2018**, *1*, 763.
[32] W. Wang, Y. Shi, C. Zhang, S. Hong, L. Shi, J. Chang, R. Li, Y. Jin, C. Ong, S. Zhuo, P. Wang, *Nat. Commun.* **2019**, *10*, 3012.
[33] P. Wang, *Environ. Sci.: Nano* **2018**, *5*, 1078.
[34] C. Zhang, H.-Q. Liang, Z.-K. Xu, Z. Wang, *Adv. Sci.* **2019**, *6*, 1900883.
[35] A. Deshmukh, C. Boo, V. Karanikola, S. Lin, A. P. Straub, T. Tong, D. M. Warsinger, M. Elimelech, *Energy Environ. Sci.* **2018**, *11*, 1177.
[36] Z. Wang, T. Horseman, A. P. Straub, N. Y. Yip, D. Li, M. Elimelech, S. Lin, *Sci. Adv.* **2019**, *5*, eaax0763.
[37] Y.-S. Jun, X. Wu, D. Ghim, Q. Jiang, S. Cao, S. Singamaneni, *Acc. Chem. Res.* **2019**, *52*, 1215.
[38] R. Long, Y. Li, L. Song, Y. Xiong, *Small* **2015**, *11*, 3873.
[39] M. L. Brongersma, N. J. Halas, P. Nordlander, *Nat. Nanotechnol.* **2015**, *10*, 25.
[40] D. J. de Aberasturi, A. B. Serrano-Montes, L. M. Liz-Marzán, *Adv. Opt. Mater.* **2015**, *3*, 602.
[41] C. M. Hessel, V. P. Pattani, M. Rasch, M. G. Panthani, B. Koo, J. W. Tunnell, B. A. Korgel, *Nano Lett.* **2011**, *11*, 2560.
[42] J. R. Vélez-Cordero, J. Hernández-Cordero, *Int. J. Therm. Sci.* **2015**, *96*, 12.
[43] A. Amri, Z. T. Jiang, T. Pryor, C.-Y. Yin, S. Djordjevic, *Renewable Sustainable Energy Rev.* **2014**, *36*, 316.
[44] A. Politano, P. Argurio, G. Di Profio, V. Sanna, A. Cupolillo, S. Chakraborty, H. A. Arafat, E. Curcio, *Adv. Mater.* **2017**, *29*, 1603504.
[45] J. Wu, K. R. Zodrow, P. B. Szemraj, Q. Li, *J. Mater. Chem. A* **2017**, *5*, 23712.
[46] X. Wu, Q. Jiang, D. Ghim, S. Singamaneni, Y.-S. Jun, *J. Mater. Chem. A* **2018**, *6*, 18799.
[47] L. Zhu, M. Gao, C. K. N. Peh, G. W. Ho, *Nano Energy* **2019**, *57*, 507.
[48] B. Gong, H. Yang, S. Wu, J. Yan, K. Cen, Z. Bo, K. K. Ostrikov, *ACS Sustainable Chem. Eng.* **2019**, *7*, 20151.
[49] E. K. Summers, J. H. Lienhard, *Desalination* **2013**, *330*, 100.
[50] M. Gao, L. Zhu, C. K. Peh, G. W. Ho, *Energy Environ. Sci.* **2019**, *12*, 841.
[51] W. Shang, T. Deng, *Nat. Energy* **2016**, *1*, 16133.
[52] S. Hong, Y. Shi, R. Li, C. Zhang, Y. Jin, P. Wang, *ACS Appl. Mater. Interfaces* **2018**, *10*, 28517.
[53] Y. Ito, Y. Tanabe, J. Han, T. Fujita, K. Tanigaki, M. Chen, *Adv. Mater.* **2015**, *27*, 4302.
[54] P. D. Dongare, A. Alabastri, S. Pedersen, K. R. Zodrow, N. J. Hogan, O. Neumann, J. Wu, T. Wang, A. Deshmukh, M. Elimelech, Q. Li, P. Nordlander, N. J. Halas, *Proc. Natl. Acad. Sci. USA* **2017**, *114*, 6936.
[55] P. D. Dongare, A. Alabastri, O. Neumann, P. Nordlander, N. J. Halas, *Proc. Natl. Acad. Sci. USA* **2019**, *116*, 13182.
[56] S. Cao, X. Wu, Y. Zhu, R. Gupta, A. Tan, Z. Wang, Y.-S. Jun, S. Singamaneni, *J. Mater. Chem. A* **2020**, *8*, 5147.
[57] Y. Wang, C. Wang, X. Song, M. Huang, S. K. Megarajan, S. F. Shaukat, H. Jiang, *J. Mater. Chem. A* **2018**, *6*, 9874.
[58] X. Li, J. Li, J. Lu, N. Xu, C. Chen, X. Min, B. Zhu, H. Li, L. Zhou, S. Zhu, T. Zhang, J. Zhu, *Joule* **2018**, *2*, 1331.
[59] H. Song, Y. Liu, Z. Liu, M. H. Singer, C. Li, A. R. Cheney, D. Ji, L. Zhou, N. Zhang, X. Zeng, Z. Bei, Z. Yu, S. Jiang, Q. Gan, *Adv. Sci.* **2018**, *5*, 1800222.
[60] F. Jiang, H. Liu, Y. Li, Y. Kuang, X. Xu, C. Chen, H. Huang, C. Jia, X. Zhao, E. Hitz, Y. Zhou, R. Yang, L. Cui, L. Hu, *ACS Appl. Mater. Interfaces* **2018**, *10*, 1104.
[61] Y. Wang, X. Wu, B. Shao, X. Yang, G. Owens, H. Xu, *Sci. Bull.* **2020**, *65*, 1380.
[62] Y. Shi, R. Li, Y. Jin, S. Zhuo, L. Shi, J. Chang, S. Hong, K.-C. Ng, P. Wang, *Joule* **2018**, *2*, 1171.
[63] Y. Z. Tan, H. Wang, L. Han, M. B. Tanis-Kanbur, M. V. Pranav, J. W. Chew, *J. Membr. Sci.* **2018**, *565*, 254.
[64] S. Lin, N. Y. Yip, M. Elimelech, *J. Membr. Sci.* **2014**, *453*, 498.
[65] E. K. Summers, H. A. Arafat, J. H. Lienhard, *Desalination* **2012**, *290*, 54.
[66] J. Swaminathan, H. W. Chung, D. M. Warsinger, J. H. Lienhard V, *Appl. Energy* **2018**, *211*, 715.
[67] M. A. E.-R. Abu-Zeid, Y. Zhang, H. Dong, L. Zhang, H.-L. Chen, L. Hou, *Desalination* **2015**, *356*, 1.
[68] G. Zaragoza, J. A. Andrés-Mañas, A. Ruiz-Aguirre, *npj Clean Water* **2018**, *1*, 20.
[69] S. Linic, U. Aslam, C. Boerigter, M. Morabito, *Nat. Mater.* **2015**, *14*, 567.
[70] L. Zhu, M. Gao, C. K. N. Peh, G. W. Ho, *Mater. Horiz.* **2018**, *5*, 323.
[71] H. Liu, J. Zhou, C. Wu, C. Wang, Y. Zhang, D. Liu, Y. Lin, H. Jiang, L. Song, *ACS Sustainable Chem. Eng.* **2018**, *6*, 2911.
[72] C. Chen, Y. Li, J. Song, Z. Yang, Y. Kuang, E. Hitz, C. Jia, A. Gong, F. Jiang, J. Y. Zhu, B. Yang, J. Xie, L. Hu, *Adv. Mater.* **2017**, *29*, 1701756.
[73] Y. Li, T. Gao, Z. Yang, C. Chen, W. Luo, J. Song, E. Hitz, C. Jia, Y. Zhou, B. Liu, B. Yang, L. Hu, *Adv. Mater.* **2017**, *29*, 1700981.
[74] P. Zhang, J. Li, L. Lv, Y. Zhao, L. Qu, *ACS Nano* **2017**, *11*, 5087.
[75] Z. Liu, H. Song, D. Ji, C. Li, A. Cheney, Y. Liu, N. Zhang, X. Zeng, B. Chen, J. Gao, Y. Li, X. Liu, D. Aga, S. Jiang, Z. Yu, Q. Gan, *Global Challenges* **2017**, *1*, 1600003.
[76] Q. Fang, T. Li, Z. Chen, H. Lin, P. Wang, F. Liu, *ACS Appl. Mater. Interfaces* **2019**, *11*, 10672.
[77] N. Xu, X. Hu, W. Xu, X. Li, L. Zhou, S. Zhu, J. Zhu, *Adv. Mater.* **2017**, *29*, 1606762.
[78] C. Jia, Y. Li, Z. Yang, G. Chen, Y. Yao, F. Jiang, Y. Kuang, G. Pastel, H. Xie, B. Yang, S. Das, L. Hu, *Joule* **2017**, *1*, 588.
[79] P. Zhang, Q. Liao, T. Zhang, H. Cheng, Y. Huang, C. Yang, C. Li, L. Jiang, L. Qu, *Nano Energy* **2018**, *46*, 415.
[80] H. Geng, Q. Xu, M. Wu, H. Ma, P. Zhang, T. Gao, L. Qu, T. Ma, C. Li, *Nat. Commun.* **2019**, *10*, 1512.
[81] K.-K. Liu, Q. Jiang, S. Tadepalli, R. Raliya, P. Biswas, R. R. Naik, S. Singamaneni, *ACS Appl. Mater. Interfaces* **2017**, *9*, 7675.
[82] M. Gao, C. K. Peh, H. T. Phan, L. Zhu, G. W. Ho, *Adv. Energy Mater.* **2018**, *8*, 1800711.
[83] Z. Wang, Y. Liu, P. Tao, Q. Shen, N. Yi, F. Zhang, Q. Liu, C. Song, D. Zhang, W. Shang, T. Deng, *Small* **2014**, *10*, 3234.
[84] M. Zhu, Y. Li, F. Chen, X. Zhu, J. Dai, Y. Li, Z. Yang, X. Yan, J. Song, Y. Wang, E. Hitz, W. Luo, M. Lu, B. Yang, L. Hu, *Adv. Energy Mater.* **2018**, *8*, 1701028.
[85] J. Wang, Y. Li, L. Deng, N. Wei, Y. Weng, S. Dong, D. Qi, J. Qiu, X. Chen, T. Wu, *Adv. Mater.* **2017**, *29*, 1603730.
[86] X. Chen, L. Liu, P. Y. Yu, S. S. Mao, *Science* **2011**, *331*, 746.
[87] J. M. Luther, P. K. Jain, T. Ewers, A. P. Alivisatos, *Nat. Mater.* **2011**, *10*, 361.
[88] A. Comin, L. Manna, *Chem. Soc. Rev.* **2014**, *43*, 3957.

[89] C. Zhang, C. Yan, Z. Xue, W. Yu, Y. Xie, T. Wang, *Small* **2016**, *12*, 5320.
[90] R. Li, L. Zhang, L. Shi, P. Wang, *ACS Nano* **2017**, *11*, 3752.
[91] S. Ishii, R. P. Sugavaneshwar, T. Nagao, *J. Phys. Chem. C* **2016**, *120*, 2343.
[92] M. Kaur, S. Ishii, S. L. Shinde, T. Nagao, *ACS Sustainable Chem. Eng.* **2017**, *5*, 8523.
[93] X. Zhou, F. Zhao, Y. Guo, B. Rosenberger, G. Yu, *Sci. Adv.* **2019**, *5*, eaaw5484.
[94] Y. Pang, J. Zhang, R. Ma, Z. Qu, E. Lee, T. Luo, *ACS Energy Lett.* **2020**, *5*, 437.
[95] H. Ye, X. Li, L. Deng, P. Li, T. Zhang, X. Wang, B. S. Hsiao, *Ind. Eng. Chem. Res.* **2019**, *58*, 3269.
[96] E. H. Ang, Y. Z. Tan, J. W. Chew, *J. Mater. Chem. A* **2019**, *7*, 10206.
[97] D. H. Seo, S. Pineda, Y. C. Woo, M. Xie, A. T. Murdock, E. Y. M. Ang, Y. Jiao, M. J. Park, S. I. Lim, M. Lawn, F. F. Borghi, Z. J. Han, S. Gray, G. Millar, A. Du, H. K. Shon, T. Y. Ng, K. Ostrikov, *Nat. Commun.* **2018**, *9*, 683.
[98] C. Boo, J. Lee, M. Elimelech, *Environ. Sci. Technol.* **2016**, *50*, 8112.
[99] Z. Zhu, Y. Xu, Y. Luo, W. Wang, X. Chen, *J. Mater. Chem. A* **2021**, *9*, 702.
[100] M. Tomaszewska, in *Encyclopedia of Membranes* (Eds: E. Drioli, L. Giorno), Springer Berlin Heidelberg, Berlin **2016**, p. 33.
[101] L. D. Tijing, Y. C. Woo, J.-S. Choi, S. Lee, S.-H. Kim, H. K. Shon, *J. Membr. Sci.* **2015**, *475*, 215.
[102] K. W. Lawson, D. R. Lloyd, *J. Membr. Sci.* **1997**, *124*, 1.
[103] D. Rice, S. J. Ghadimi, A. C. Barrios, S. Henry, W. S. Walker, Q. Li, F. Perreault, *Environ. Sci. Technol.* **2020**, *54*, 2548.
[104] L. E. Armstrong, E. C. Johnson, *Nutrients* **2018**, *10*, 1928.
[105] P. Yang, K. Liu, Q. Chen, J. Li, J. Duan, G. Xue, Z. Xu, W. Xie, J. Zhou, *Energy Environ. Sci.* **2017**, *10*, 1923.
[106] M. Gao, P. K. N. Connor, G. W. Ho, *Energy Environ. Sci.* **2016**, *9*, 3151.
[107] G. Xue, Y. Xu, T. Ding, J. Li, J. Yin, W. Fei, Y. Cao, J. Yu, L. Yuan, L. Gong, J. Chen, S. Deng, J. Zhou, W. Guo, *Nat. Nanotechnol.* **2017**, *12*, 317.
[108] F. L. Meng, M. Gao, T. Ding, G. Yilmaz, W. L. Ong, G. W. Ho, *Adv. Funct. Mater.* **2017**, *30*, 2002867.
[109] L. Zhu, T. Ding, M. Gao, C. K. N. Peh, G. W. Ho, *Adv. Energy Mater.* **2019**, *9*, 1900250.
[110] G. Liu, T. Chen, J. Xu, G. Li, K. Wang, *J. Mater. Chem. A* **2020**, *8*, 513.
[111] Q. Zhang, S. Chen, Z. Fu, H. Yu, X. Quan, *Nano Energy* **2020**, *76*, 105060.
[112] Q. Shen, Z. Ning, B. Fu, S. Ma, Z. Wang, L. Shu, L. Zhang, X. Wang, J. Xu, P. Tao, C. Song, J. Wu, T. Deng, W. Shang, *J. Mater. Chem. A* **2019**, *7*, 6514.

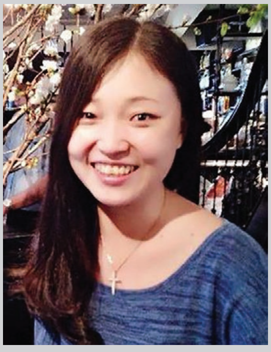

Minmin Gao received her B. Eng. (Hons.) degree in Electrical Engineering from the National University of Singapore (NUS) in 2012, as well as her Ph.D. in 2016 under the supervision of Prof. Ghim Wei Ho. Her research interest currently focuses on nanomaterials for clean energy generation, photothermal water evaporation, and photocatalytic applications.

Connor Peh received his B. Eng. (Hons.) and Ph.D. degrees from the National University of Singapore in 2009 and 2016, respectively. He did his postdoctoral research in Prof Ho Ghim Wei's group. His research interests primarily focus on clean energy generation, photocatalytic and photoelectrochemical water splitting, and the development of materials to harness sunlight in various forms.

Fan Lu Meng received his Ph.D. degree in Materials Science at the Jilin University of China and Inorganic Chemistry at the Changchun Institute of Applied Chemistry, Chinese Academy of Sciences in 2017. He is now a research fellow at the Department of Electrical & Computer Engineering at the National University of Singapore (NUS). His current interests include the synthesis and characterization of nanostructures for clean energy conversion reactions.

Ghim Wei Ho received her Ph.D. in Semiconductor Nanostructures at the Nanoscience Centre, University of Cambridge in 2006. She is a professor at the Department of Electrical and Computer Engineering at the National University of Singapore (NUS). She leads the sustainable smart solar system research group working on fundamental and applied research on nanosystems with emerging low dimensional nanomaterials, interfacial interactions, and hybridized functionalities for energy, environment, electronics, and healthcare.